REPORT DOCUMENTATION PAGE

Form Approved OMB NO. 0704-0188

1. REPORT DATE (DD-MM-YYYY)	2. REPORT TYPE	3. DATES COVERED (From - To)
	New Reprint	-

4. TITLE AND SUBTITLE

Observation of Distinct Surface AlIV Sites and Phosphonate Binding Modes in ?-Alumina and Concrete by High-Field 27Al and 31P MAS NMR

5a. CONTRACT NUMBER

W911NF-07-1-0053

5b. GRANT NUMBER

5c. PROGRAM ELEMENT NUMBER

BD2256

6. AUTHORS

George W. Wagner, Roderick A. Fry

5d. PROJECT NUMBER

5e. TASK NUMBER

5f. WORK UNIT NUMBER

7. PERFORMING ORGANIZATION NAMES AND ADDRESSES

New York Structural Biology
RRL 317B
1275 York Ave.
New York, NY 10021 -6094

8. PERFORMING ORGANIZATION REPORT NUMBER

9. SPONSORING/MONITORING AGENCY NAME(S) AND ADDRESS(ES)

U.S. Army Research Office
P.O. Box 12211
Research Triangle Park, NC 27709-2211

10. SPONSOR/MONITOR'S ACRONYM(S)

ARO

11. SPONSOR/MONITOR'S REPORT NUMBER(S)

51980-CH.4

12. DISTRIBUTION AVAILIBILITY STATEMENT

Approved for public release; distribution is unlimited.

13. SUPPLEMENTARY NOTES

The views, opinions and/or findings contained in this report are those of the author(s) and should not contrued as an official Department of the Army position, policy or decision, unless so designated by other documentation.

14. ABSTRACT

High loadings of nerve agent-related phosphonic acids adsorbed on ?-Al2O3 and concrete examined by 31P MAS NMR and high-field 27Al MAS NMR reveal the presence of several phosphonate-surface binding modes and greatly improved resolution of multiple AlIV sites. Some of the resolved AlIV sites are sensitive to surface hydroxylation/dehydroxylation are attributed to surface AlIV-OH groups (apparently having been observed for the first time). Although the number of surface AlIV sites detected by high-field 27Al MAS NMR

15. SUBJECT TERMS

31PMAS NMR, 27Al MAS NMR, VX, Nerve agent, decontamination

16. SECURITY CLASSIFICATION OF:			17. LIMITATION OF ABSTRACT	15. NUMBER OF PAGES	19a. NAME OF RESPONSIBLE PERSON
a. REPORT	b. ABSTRACT	c. THIS PAGE			Michael Goger
UU	UU	UU	UU		19b. TELEPHONE NUMBER: 212-939-0660

Report Title

Observation of Distinct Surface AlIV Sites and Phosphonate Binding Modes in ?-Alumina and Concrete by High-Field 27Al and 31P MAS NMR

ABSTRACT

High loadings of nerve agent-related phosphonic acids adsorbed on ?-Al2O3 and concrete examined by 31P MAS NMR and high-field 27Al MAS NMR reveal the presence of several phosphonate-surface binding modes and greatly improved resolution of multiple AlIV sites. Some of the resolved AlIV sites are sensitive to surface hydroxylation/dehydroxylation are attributed to surface AlIV-OH groups (apparently having been observed for the first time). Although the number of surface AlIV sites detected by high-field 27Al MAS NMR (three) is in agreement with current surface models, their dehydroxylation behavior does not entirely concur with proposed dehydroxylation mechanisms. The various phosphonate-alumina surface species detected by 31P MAS NMR are consistent with those previously observed by IR techniques. In concrete, the formation of an aluminophosphonate species is directly observed, consistent with the recalcitrant extraction behavior exhibited by adsorbed phosphonates in environmental matrices.

REPORT DOCUMENTATION PAGE (SF298)
(Continuation Sheet)

Continuation for Block 13

ARO Report Number 51980.4-CH
Observation of Distinct Surface AlIV Sites and P ...

Block 13: Supplementary Note

Approved for public release; distribution is unlimited.

Observation of Distinct Surface Al_{IV} Sites and Phosphonate Binding Modes in γ-Alumina and Concrete by High-Field ^{27}Al and ^{31}P MAS NMR

George W. Wagner*,† and Roderick A. Fry‡,§

U.S. Army Edgewood Chemical Biological Center, Attn: AMSRD-ECB-RT-PF, Aberdeen Proving Ground, Maryland 21010-5424, and SAIC, Gunpowder Branch, P.O. Box 68, Aberdeen Proving Ground, Maryland 21010-0068

Received: March 19, 2009; Revised Manuscript Received: May 28, 2009

High loadings of nerve agent-related phosphonic acids adsorbed on γ-Al_2O_3 and concrete examined by ^{31}P MAS NMR and high-field ^{27}Al MAS NMR reveal the presence of several phosphonate−surface binding modes and greatly improved resolution of multiple Al_{IV} sites. Some of the resolved Al_{IV} sites are sensitive to surface hydroxylation/dehydroxylation are attributed to surface Al_{IV}−OH groups (apparently having been observed for the first time). Although the number of surface Al_{IV} sites detected by high-field ^{27}Al MAS NMR (three) is in agreement with current surface models, their dehydroxylation behavior does not entirely concur with proposed dehydroxylation mechanisms. The various phosphonate−alumina surface species detected by ^{31}P MAS NMR are consistent with those previously observed by IR techniques. In concrete, the formation of an aluminophosphonate species is directly observed, consistent with the recalcitrant extraction behavior exhibited by adsorbed phosphonates in environmental matrices.

Introduction

Nerve agents GB (isopropyl methylphosphonofluoridate), GD (pinacolyl methylphosphonofluoridate), and VX [*O*-ethyl-*S*-(2-diisopropylamino)ethyl methylphosphonothioate] hydrolyze on metal oxides[1−5] and concrete,[6−8] forming their corresponding phosphonic acids (Scheme 1). Previous work examining these reactions on γ-Al_2O_3 by ^{31}P and ^{27}Al MAS NMR[3] showed binding of these species to the alumina surface (surface-complexes **4** and **5**; Scheme 3 below) the formation of discrete aluminophosphonate species (**6** and **7**; Scheme 3 below) via surface erosion and the secondary hydrolysis of VX-derived ethyl methylphosphonate (EMPA) to methylphosphonate (MPA). Isopropyl methylphosphonate (IMPA) and pinacolyl methylphosphonate (PMPA), the hydrolysis products of GB and GD, respectively, were not observed to undergo secondary hydrolysis.[3] In the present work, examining higher surface loadings and utilizing high-field NMR affords greater detail concerning the manner in which phosphonates interact and bind to alumina and concrete surfaces, and the nature of the γ-Al_2O_3 surface itself.

Ultrahigh magnetic field (21.1 T) ^{27}Al MAS NMR spectra have already been reported by Peden et al.[9] for γ-Al_2O_3 where samples calcined at 500 °C showed baseline-separation of resonances for tetrahedral (Al_{IV}, 72.8 ppm), pentacoordinated (Al_V, 38 ppm), and octahedral (Al_{VI}, 13.8 ppm) aluminum sites; the Al_V sites evidently residing exclusively on the surface.[10] Massiot et al.[11] have noted that Al_V sites are an anomaly within the γ-Al_2O_3 defective spinel structure (composed of Al_{IV} and Al_{VI} elementary units); thus, Al_V sites, or lack thereof, is an indicator as to the amount of structural disorder.

Calcination at 500 °C removes physisorbed water and hydroxyls on adjacent Al sites (most easily removed; perhaps as much as 90.4% of the surface hydroxyls[12]), leaving primarily isolated surface hydroxyls which are only slowly removed at higher temperatures.[13] Thus, ultrahigh magnetic field studies to date have reported ^{27}Al MAS NMR spectra for very *dehydroxylated* γ-Al_2O_3 surfaces, demonstrating improved resolution between each class of Al site (Al_{IV}, Al_V, Al_{VI}). However, as shown below, ultrahigh field ^{27}Al MAS NMR is of further use for studying *hydroxylated* γ-Al_2O_3 surfaces, enabling resolution of distinct bulk and surface Al_{IV} sites, the latter exhibiting dramatic changes during dehydroxylation.

Experimental Section

Materials and Methods. Samples were prepared by adding measured amounts of neat liquid (PMPA, IMPA, EMPA) and solid (MPA) phosphonic acids (Aldrich) directly to γ-Al_2O_3 (Selexsorb CDX, Alcoa) and (crushed) concrete. Solid methylphosphonic acid (Aldrich) was physically mixed with γ-Al_2O_3 using a spatula. The composition of the concrete has been previously described.[14] XRF analysis (Clarkson Laboratory and Supply, Inc.) showed an alumina content of ca. 10% (see Supporting Information).

NMR. ^{31}P and ^{27}Al MAS NMR spectra were obtained using Varian Unityplus 300, INOVA 400 and 600, and Bruker AVANCE 500, 750, and 900 NMR spectrometers. Direct polarization was employed for all spectra. Spectra were referenced to 85% H_3PO_4 (^{31}P, 0 ppm) and 1 M $AlCl_3$ or 0.1 M $Al(NO_3)_3 \cdot 9H_2O$ in H_2O (^{27}Al, 0 ppm; both solutions yielded the exact same shift).

Results and Discussion

High-Field ^{27}Al MAS NMR of γ-Al_2O_3. Figure 1 shows ^{27}Al MAS NMR spectra obtained for the same commercial sample of γ-Al_2O_3 utilized in ref 3 at various magnetic fields and hydoxylated at ambient humidity (see below). As expected, dramatic sharpening of both the Al_{IV} (four-coordinate, tetrahedral sites; ca. 60 ppm) and Al_{VI} (six-coordinate, octahedral sites; ca. 10 ppm) is observed on moving to higher field as second-

* To whom correspondence should be addressed. E-mail: george.wagner@us.army.mil.
† U.S. Army Edgewood Chemical Biological Center.
‡ SAIC.
§ Current address: U.S. Army Edgewood Chemical Biological Center, Attn: AMSRD-ECB-RT-CM, Aberdeen Proving Ground, MD 21010-5424.

10.1021/jp902474z CCC: $40.75
Published on Web 07/01/2009

SCHEME 1

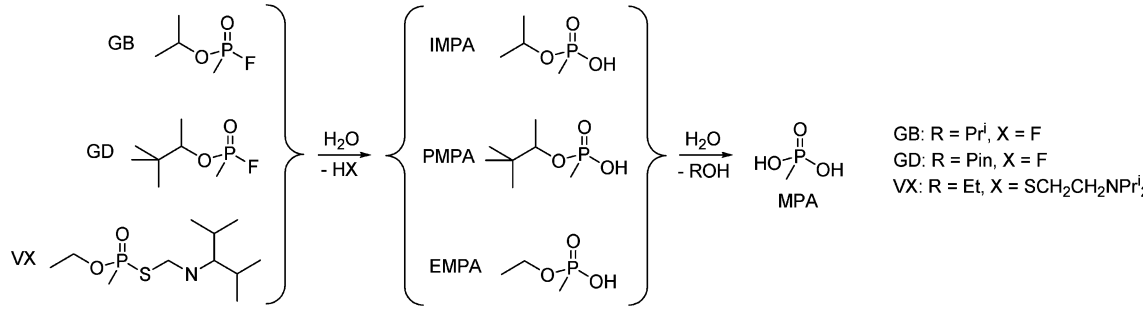

order quadrupolar (broadening) effects become subordinate to the dominant NMR Zeeman interaction.[15] For the Al_{VI} sites, especially marked sharpening occurs between 9.4 and 14 T with minor, further sharpening at the higher fields. (The large difference in resolution between 9.4 and 14 T is not due to the disparity in spinning speed, i.e., 4300 vs 8000 Hz, as variable spinning experiments performed at 9.4 and 17 T from 5000 to 17 000 Hz showed little effect on the linewidths of either the Al_{IV} or Al_{VI} resonances (see Supporting Information).) Also at the higher fields, a small signal for Al_V (pentacoordinated sites; ca. 35 ppm)[9,10,16] (see below) is able to be resolved between the much more intense Al_{IV} and Al_{VI} peaks. However, it is the Al_{IV} sites which benefit most from the highest 21 T field strength as three separate sites become clearly resolved at 68.4, 60.3, and 57.5 ppm (a shoulder; still somewhat visible at 17.5 and 14 T).

Dehydroxylation Behavior of γ-Al_2O_3. Figure 2 shows 21-T ^{27}Al MAS NMR spectra obtained for the γ-Al_2O_3 before and after partial dehydroxylation at 400 °C. The Al_V regions near 35 ppm are enhanced in the insets for each spectrum. Tentative assignments of the multiple Al_{IV} peaks resolved in Figure 2 are discussed below. Partial dehydroxylation results in the disappearance of the two overlapping Al_{IV} peaks at 60.3 and 57.5 ppm, apparently being replaced by a much broader peak at 55.9 ppm. The remaining Al_{IV} peak at 68.4 ppm is only slightly broadened by the water-loss and is presumably due primarily to internal (not surface) Al_{IV} sites which tend to comprise about 25% of the total Al in γ-Al_2O_3.[17] These results are in partial agreement with Coster et al.[18] who previously observed two separate Al_{IV} peaks at 11.7 T in dehydrated γ-Al_2O_3, which are remarkably similar to the present 68.4 and 55.9 ppm peaks, but resolved only a single Al_{IV} in the hydrated material (presumably due to peak overlapping/decreased resolution at the lower field strength employed). For the Al_V peak no major intensity (peak area) change is observed, although subtle shifting of its shift from 35 (hydroxylated surface) to 33 ppm (dehydroxylated surface) suggests some awareness of nearby surface hydroxyls. The insensitivity of Al_V sites to drying/dehydroxylation (200 °C) has very recently been noted by Skibsted et al.;[19] thus, the Al_V sites do not appear to be directly involved in the dehydroxylation process observed at these temperatures. Like the Al_{IV} sites, the Al_{VI} peak at 10.2 ppm is also broadened by the loss of water, consistent with the observations of Morris and Ellis.[20] Data obtained at 14 T (not shown) show that besides the broadening, partial dehroxylation at 400 °C results in intensity (peak area) losses for both the Al_{VI} peak and Al_{IV} peaks (total) of 16% and 19%, respectively. Some of this decrease in intensity (peak area) may simply be due to attendant changes in second-order quadrupolar effects which could severely broaden resonances, adversely impacting their intensity. (Gan

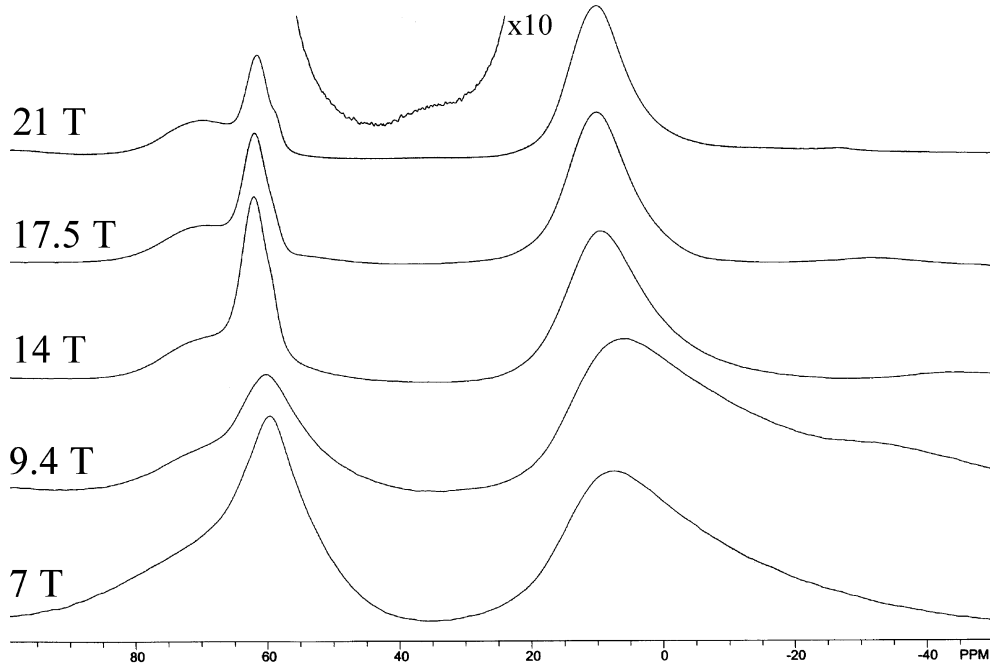

Figure 1. ^{27}Al MAS NMR spectra obtained for γ-Al_2O_3 at 7 (ν_r = 5600 Hz), 9.4 (ν_r = 4300 Hz), 14 (ν_r = 8000 Hz), 17.5 (ν_r = 8000 Hz), and 21 T (ν_r = 20 000 Hz). Inset shows enhanced (10×) Al_V region for the 21 T spectrum.

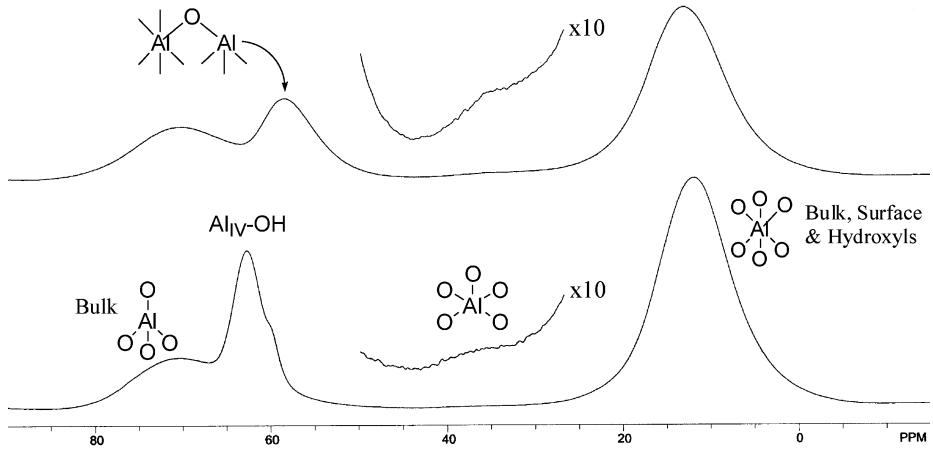

Figure 2. ^{27}Al MAS NMR (21 T, ν_r = 20 000 Hz) spectra obtained for as-received (hydrated, bottom) and partially dehydrated (400 °C, top) γ-Al_2O_3.

SCHEME 2

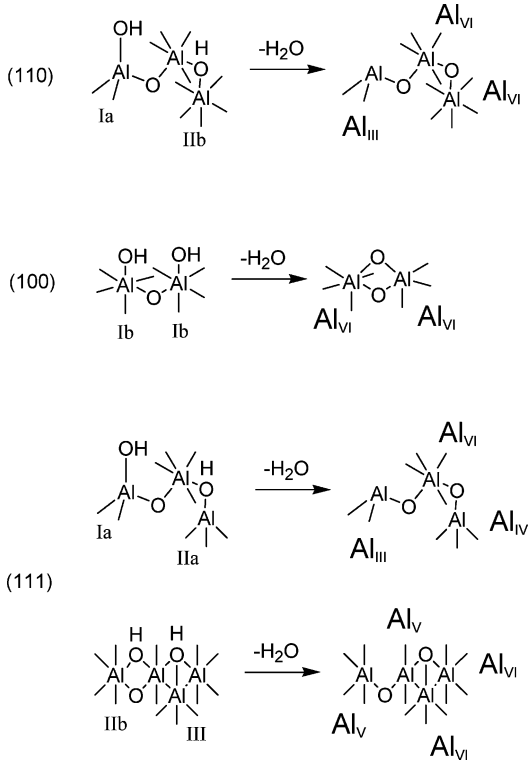

et al.[15] have shown that quantitative ^{27}Al MAS NMR spectra may be obtained when second-order quadrupolar effects are small compared to the magnetic field strength.)

Comparison of High-Field ^{27}Al MAS NMR Observations with γ-Al_2O_3 Surface Model. Knozinger and Ratnasamy[21] proposed five types of surface hydroxyl groups on γ-Al_2O_3, which reside on the various available crystal faces, and further suggested preferred dehydroxylation pathways as shown in Scheme 2. Starting with the (110) face, dehydroxylation of the adjacent Ia and IIb sites would result in the loss of a Al_{IV}-Ia site, forming a Al_{III} site and two modified Al_{VI}-IIb sites. This mechanism is in agreement with the disappearance of one of the two resolved Al_{IV} sites (60.3 or 57.5 ppm), both of which are assigned to Al_{IV}−OH groups in terminal Ia and/or bridging IIa sites (see below). Modification of the bonding in the Al_{VI} sites should be reflected in a change in line width of the Al_{VI} peak at 10 ppm as the bonding and, hence, the electric field gradient around the Al_{VI} sites changes. This is indeed the case as noted above for Figure 2. Although the formation of Al_{III} sites is predicted by this mechanism, they have not been observed on γ-Al_2O_3.[22] Sohlberg et al.[22] have proposed that significant rearrangement of surface sites occurs such that generated Al_{III} sites fill vacant octahedral sites. Although, this de facto conversion of Al_{IV} to Al_{VI} is consistent with the intensity-loss noted above for the Al_{IV} region, it would *increase* the intensity of the Al_{VI} peak, in opposition to the experimentally observed intensity *decrease*.

The (100) face possesses uniform Al_{VI}-Ib sites. Statistical removal of water from adjacent sites[12] would merely generate additional modified Al_{VI} sites (with the attendant line width modification of the Al_{VI} peak at 10 ppm) with no change in intensity (peak area) anticipated (ignoring second-order quadrupolar effects[15]).

For the (111) face, two possible dehydroxylation scenarios are possible. The favored mechanism is loss of water from the adjacent Ia (basic) and IIa (acidic) groups to generate a (transient?) Al_{III} site and modified Al_{IV} and Al_{VI} sites. This mechanism is also in agreement with not only the disappearance of a second Al_{IV}−OH resonance (see above) but also the emergence of the Al_{IV} peak at 55.9 ppm which can be assigned to the modified Al_{IV}-IIa site. However, the original, total intensity of the Al_{IV}−OH resonances (60.2 and 57.5 ppm) appears much too small to account for the relatively large intensity of this dehydroxylated Al_{VI} site since it should be a two-for-one swap, i.e., one Ia and one IIa would give only one modified (dehydroxylated) IIa. Again, intensity-distorting second-order quadrupole effects[15] cannot be ruled out and additional unknown surface rearrangements could be the cause of the unexpectedly large intensity of the new, dehydroxylated Al_{IV} site (see below). As mentioned above, the lost Al_{IV}-Ia would yield an additional Al_{VI} site (via relaxation of the Al_{III} into a vacant Al_{VI} site), resulting in a further addition of intensity to the Al_{VI} peak (not the experimentally observed decrease).

It is the second dehydroxylation mechanism of the (111) face which offers a possible explanation for the experimentally observed intensity decrease of the Al_{VI} sites. For this final mechanism, water-loss converts two Al_{VI} sites, one from IIb and one from III, to two Al_V sites; the remaining two Al_{VI}-III sites are merely modified (as previously discussed). Thus, this mechanism potentially accounts for observed loss in intensity of the Al_{VI} peak (10 ppm). However, comparable intensity increase in the Al_V peak region (ca. 35 ppm) is certainly not

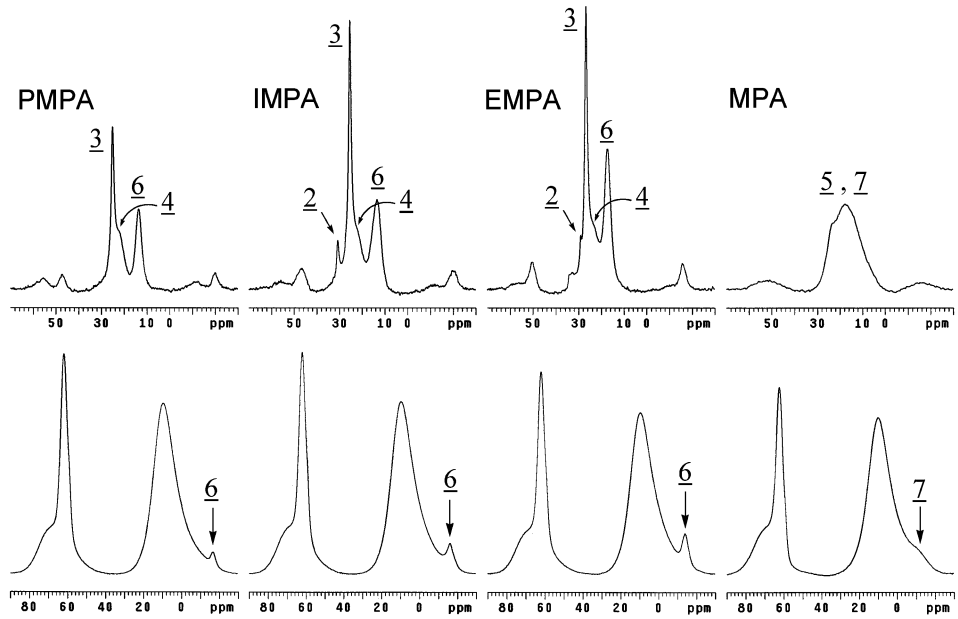

Figure 3. ^{31}P (top) and ^{27}Al (bottom) MAS NMR spectra obtained for phosphonates adsorbed on γ-Al_2O_3 (see text).

SCHEME 3

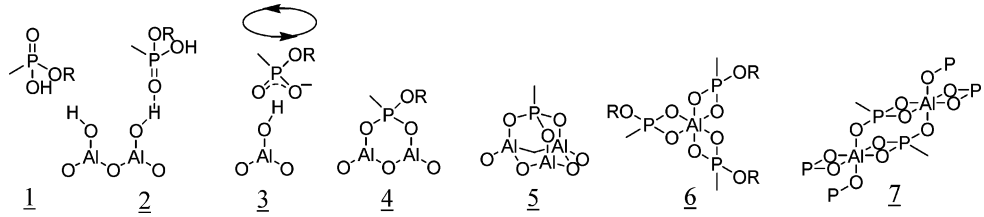

observed in the upper spectrum of Figure 2. Although a severe change in second-order quadrupolar effects[15] precluding their detection and/or adequate quantitation cannot be ruled out, a more plausible explanation is relaxation of these newly formed *surface* Al_V sites to either Al_{VI} or Al_{IV} sites in a manner analogous to that proposed by Sohlberg et al.[16] for Al_{III} sites. It is important to note that potential conversion of Al_V to Al_{IV} could account for the larger-than-expected nature of the 55.9 ppm peak detected in the partially dehydroxylated material.

The above discussion merely attempts to match some of the experimental details provided by this preliminary high-field ^{27}Al MAS NMR data to an existing γ-Al_2O_3 surface model. Clearly, additional work is needed to reconcile surface models with the dehydroxylation behavior of γ-Al_2O_3 and the enhanced structural detail afforded by high-field ^{27}Al MAS NMR.

^{31}P and ^{27}Al MAS NMR of Phophonate Species on γ-Al_2O_3. ^{31}P and ^{27}Al MAS NMR spectra (both obtained at 14 T) for PMPA, IMPA, EMPA, and MPA adsorbed on γ-Al_2O_3 at respective loadings of 0.72 (13.0 wt %), 1.0 (13.8 wt %), 1.1 (13.9 wt %), and 1.1 mmol/g (10.2 wt %) are shown in Figure 3. It is readily apparent from the ^{31}P MAS NMR spectra that at these high loadings, multiple species are present. Peak assignments in Figure 3 refer to the structures shown in Scheme 3.

The binding of organophosphonates to alumina have previously been characterized by IR[23] and inelastic electron tunneling spectroscopy.[24] As shown in Scheme 3, several surface species have been identified: molecularly adsorbed (**1**, **2**), bidentate (**4**, deprotonated PMPA, IMPA, EMPA) and tridentate (**5**, deprotonated MPA). Also shown in Scheme 3 are the presumed aluminophosphonate structures **6** (PMPA, IMPA, EMPA) and **7** (MPA), which have been previously detected and characterized by ^{31}P and ^{27}Al MAS NMR.[3] These compounds[3] yield small peaks near −16 ppm in the ^{27}Al MAS NMR spectra of Figure 3. The ^{31}P MAS NMR peak assignments of **6**[3] are straightforward, as they are distinctly shifted upfield and their rigid structures yield spinning sidebands.[25] However, the peak for **7** is quite broad such that it may overlap with that of any potentially formed **5**. Since a small peak is present near 23.3 ppm for excess, loosely bound MPA, it is probable that **5** is indeed present but its peak is not resolved. Moving downfield, the first species encountered are the deprotonated bidentate surface complexes (ca. 25 ppm) which are not free to rotate and similarly exhibit spinning sidebands. Although not expressly specified by previous studies,[23,24] a second deprotonated species (ca. 26 ppm) is apparently present, as it possesses a shift similar to that of the bidentate species but is experiencing motional averaging[26] as evidenced by the lack of spinning sidebands. Therefore, this peak is assigned to a nonspecifically bound, unprotonated species (**3**) which would be able to freely rotate. For the higher-loading IMPA and EMPA samples, downfield-shifted peaks near 30 ppm are assigned to protonated, molecularly adsorbed species (**1** and/or **2**), the shifts of which are similar to the protonated species in solution. Experiments performed to titrate the surface with successively higher loadings (not shown) reveal that bidentate species **4** forms first, followed simultaneously by **3** and **6** (consistent with the need of excess acid to effect formation of the latter), and finally, once the surface capacity is apparently breached, by molecular species **1** and/or **2**.

^{31}P and ^{27}Al MAS NMR of EMPA Species in Concrete. ^{31}P and ^{27}Al MAS NMR spectra, obtained at 11.7 and 21 T, respectively, for 44 wt % EMPA adsorbed on concrete (10% alumina) are shown in Figure 4. Although not as upfield-shifted as corresponding peaks for the species on γ-Al_2O_3, two broad,

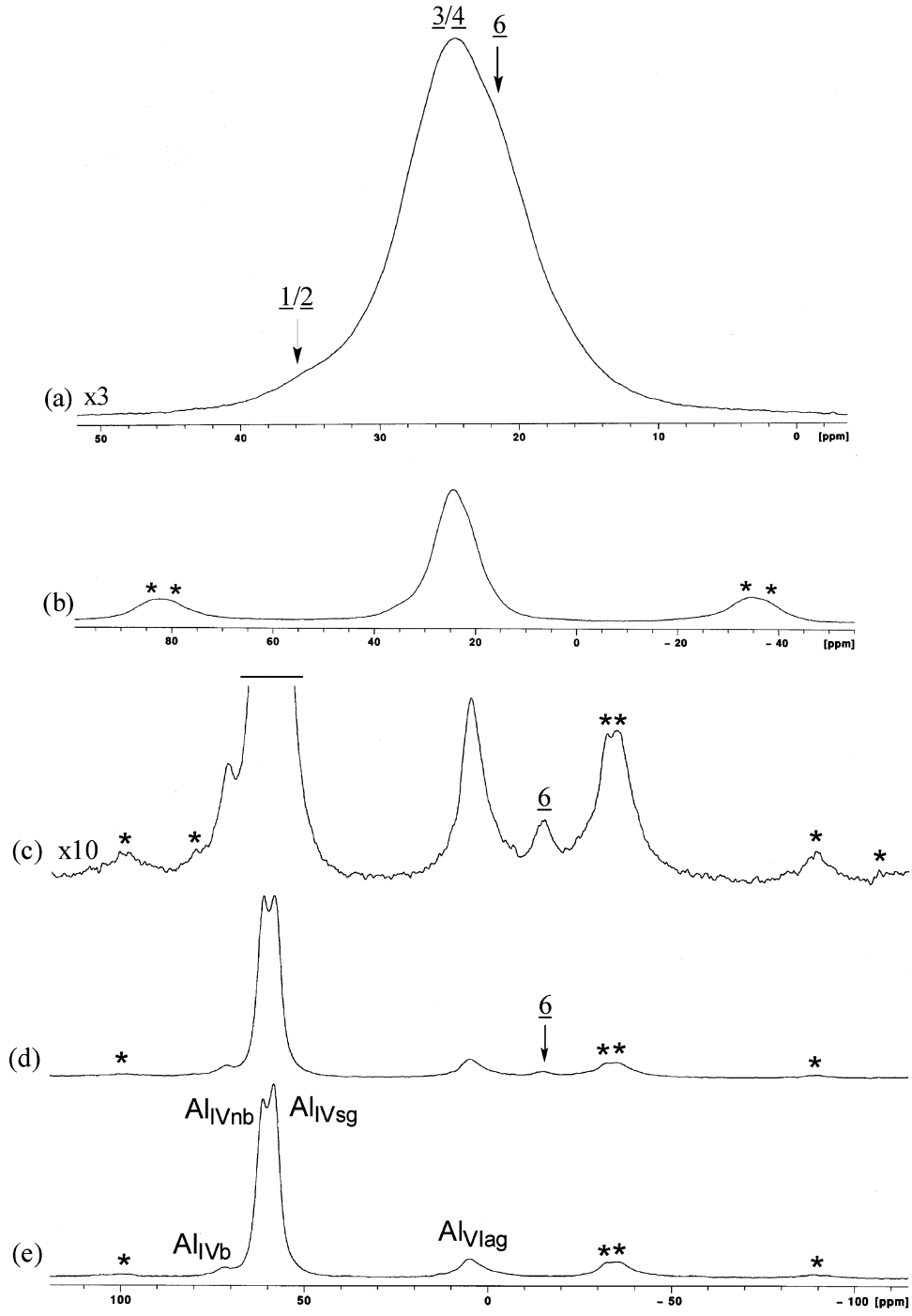

Figure 4. ^{31}P (top, a and b) and ^{27}Al (middle, c and d) MAS NMR spectra obtained for EMPA adsorbed on concrete. Spectra (a) and (c) are 3× and 10× expansions of (b) and (d), respectively. The ^{27}Al MAS NMR spectrum of the concrete prior to EMPA adsorption is shown in spectrum (e). Spinning sidebands are marked by asterisks.

overlapping peaks possessing spinning sidebands attributable to species **4** and **6** are detected at 24.6 and ca. 20 ppm, respectively (an additional small shoulder at 35 ppm is assigned to nonspecifically bound **1/2**). Although its peak cannot be resolved from the quite broad resonance of species **4**, analogous to the results for γ-Al_2O_3 (see above), species **3** is also undoubtedly present. Consistent with the observation of **6** in the ^{31}P MAS NMR spectrum, a small broad peak is detected for this species in the ^{27}Al MAS NMR spectrum at −14.8 ppm. Also present are additional background peaks due to various Al_{IV} and Al_{VI} sites present in the concrete itself, which contains about 10% alumina. Relying on previous assignments by Skibsted et al.[27] and Faucon et al.,[28] these peaks are apparently due to bridging Al_{IV} incorporated into SiO_4 chains of calcium silicate hydrates (C−S−H), 71.6 ppm; nonbridging Al_{IV} incorporated into SiO_4 chains of C−S−H, 61.6 ppm; Al_{IV} present in a silica network gel, 58.6 ppm; and Al_{VI} present in an alumina gel or calcium aluminate hydrate, 5.1 ppm (the latter two sites not incorporated in the C−S−H).

Although these results were carried out at rather high EMPA loadings (44 wt %), the fate of much smaller phosphonate loadings, perhaps more pertinent to environmental persistence, are of interest. Analogous to low-loading results previously reported for γ-Al_2O_3,[3] it is anticipated that primarily the strongest-bound species **4**, **5**, **6**, and **7** will form (additional experiments are planned to confirm these expectations). Indeed,

Kingery and Allen[29] have noted the difficulty in extracting nerve agents and/or their hydrolysis products from soil and suggested that complexation onto metal oxides may be important for environmental materials in general. This is indeed the case for concrete, especially for species such as **6** and **7** which can typically only be dissolved (extracted) by protic media at acidic pH.[3]

Conclusion

High-field ^{27}Al MAS NMR affords unprecedented resolution of various surface-related Al_{IV} sites on γ-Al_2O_3, which have apparently been reported for the first time. Whereas the number of surface Al_{IV} sites detected, three, is in agreement with the surface model of γ-Al_2O_3, their dehydration behavior is not entirely consistent with proposed surface-dehydroxylation mechanisms. For high-loadings (>10 wt %) of phosphonic acids adsorbed on γ-Al_2O_3, besides aluminophosphonate species, multiple ^{31}P MAS NMR resonances are observed reflective of several surface species attributable to both deprotonated (mono-, bi-, and tridentate) and protonated (H-bonded, free) species which have previously been observed by IR techniques. The formation of aluminophosphonate in concrete is directly detected by ^{31}P and ^{27}Al MAS NMR, consistent with the problematic extraction of phosphonic acids from environmental materials.

Acknowledgment. Work performed at New York Structural Biology Center (NYSBC) was supported under U.S. Department of Defense Grant No. W911NF0710053. The Center is a STAR center supported by the New York State Office of Science, Technology, and Academic Research. NMR resources supported by NIH P41 GM66334. 900 MHz NMR spectrometers were purchased with funds from NIH, USA, the Keck Foundation, New York State, and the NYC Economic Development Coporation. Assistance with the high-field ^{27}Al MAS NMR work by Dr. Boris Itin, NYSBC, is gratefully acknowledged, as are helpful discussions with Dr. Carol A. S. Brevett, SAIC, regarding compositions of concrete and their interaction with G-agents.

Supporting Information Available: Mercury intrusion porosimetry and XRF analysis of concrete;^{27}Al MAS NMR spectra. This material is available free of charge via the Internet at http://pubs.acs.org.

References and Notes

(1) Wagner, G. W.; Bartram, P. W.; Koper, O.; Klabunde, K. J. *J. Phys. Chem. B* **1999**, *103*, 3225–3228.

(2) Wagner, G. W.; Koper, O.; Lucas, E.; Decker, S.; Klabunde, K. J. *J. Phys. Chem. B* **2000**, *104*, 5118–5123.

(3) Wagner, G. W.; Procell, L. R.; O'Connor, R. J.; Munavalli, S.; Carnes, C. L.; Kapoor, P. N.; Klabunde, K. J. *J. Am. Chem. Soc.* **2001**, *123*, 1636–1644.

(4) Wagner, G. W.; Procell, L. R.; Munavalli, S. *J. Phys. Chem. C* **2007**, *111*, 17564–17569.

(5) Wagner, G. W.; Chen, Q.; Wu, Y. *J. Phys. Chem. C* **2008**, *112*, 11901–11906.

(6) Wagner, G. W.; O'Connor, R. J.; Procell, L. R. *Langmuir* **2001**, *17*, 4336–4341.

(7) Williams, J. M.; Rowland, B.; Jeffrey, M. T.; Groenewold, G. S.; Appelhans, A. D.; Gresham, G. L.; Olson, J. E. *Langmuir* **2005**, *21*, 2386–2390.

(8) Mizrahi, D. M.; Columbus, I. *Environ. Sci. Technol.* **2005**, *39*, 8931–8935.

(9) Kwak, J. H.; Hu, J.; Lukaski, A.; Kim, D. H.; Szanyi, J.; Peden, C. H. F. *J. Phys. Chem. C* **2008**, *112*, 9486–9492.

(10) Kwak, J. H.; Hu, J. Z.; Kim, D. H.; Szanyi, J.; Peden, C. H. F. *J. Catal.* **2007**, *251*, 189–194.

(11) D'Espinose de Lacaillerie, J.-B.; Fretigny, C.; Massiot, D. *J. Magn. Reson.* **2008**, *192*, 244–251.

(12) Peri, J. B. *J. Phys. Chem.* **1965**, *69*, 220–230.

(13) Fitzgerald, J. J.; Giberto, P.; Dec, S. F.; Seger, M.; Maciel, G. E. *J. Am. Chem. Soc.* **1997**, *119*, 7832–7842, and references therein.

(14) Brevett, C. A. S.; Sumpter, K. B.; Wagner, G. W.; Rice, J. S. *J. Hazard. Mater.* **2007**, *140*, 353–360.

(15) Gan, Z.; Gor'kov, P.; Cross, T. A.; Samoson, A.; Massiot, D. *J. Am. Chem. Soc.* **2002**, *124*, 5634–5635.

(16) Fitzgerald, J. J.; Piedra, G.; Dec, S. F.; Seger, M.; Maciel, G. E. *J. Am. Chem. Soc.* **1997**, *119*, 7832–7842.

(17) (a) Digne, M.; Sautet, P.; Raybaud, P.; Euzen, P.; Toulhoat, H. *J. Catal.* **2004**, *226*, 54–68. (b) Krokidis, X.; Raybaud, P.; Gobichon, A.-E.; Rebours, B.; Euzen, P.; Toulhoat, H. *J. Phys. Chem. B* **2001**, *105*, 5121–5130.

(18) Coster, D.; Blumenfeld, A. L.; Fripiat, J. J. *J. Phys. Chem.* **1994**, *98*, 6201–6211.

(19) Hausen, M. R.; Jakobsen, H. J.; Skibsted, J. *J. Phys. Chem. C* **2009**, *113*, 2475–2486.

(20) Morris, H. D.; Ellis, P. D. *J. Am. Chem. Soc.* **1989**, *111*, 6045–6049.

(21) Knozinger, H.; Ratnasamy, P. *Catal. Rev. Sci. Eng.* **1978**, *17*, 31–70.

(22) Sohlberg, K.; Pennycook, S. J.; Pantelides, S. T. *J. Am. Chem. Soc.* **1999**, *121*, 10999–11001, and references therein.

(23) Kuiper, A. E. T.; van Bokhoven, J. J. G. M.; Medema, J. *J. Catal.* **1976**, *43*, 154–167.

(24) (a) Templeton, M. K.; Weinberg, W. H. *J. Am. Chem. Soc.* **1985**, *107*, 97–108. (b) Templeton, M. K.; Weinberg, W. H. *J. Am. Chem. Soc.* **1985**, *107*, 774–779.

(25) Duncan, T. M.; Douglas, D. C. *Chem. Phys.* **1984**, *87*, 339–349.

(26) (a) Vila, A. J.; Lagier, C. M.; Wagner, G. W.; Olivieri, A. C. *J. Chem. Soc., Chem. Commun.* **1991**, 683–685. (b) Olivieri, A. C. *J. Magn. Reson.* **1990**, *88*, 1–8.

(27) Daugaard, M.; Jakobsen, H. J.; Skibsted, J. *Inorg. Chem.* **2003**, *42*, 2280–2287.

(28) Faucon, P.; Delagrave, A.; Petit, J. C.; Richet, C.; Marchand, J. M.; Zanni, H. *J. Phys. Chem. B* **1999**, *103*, 7796–7802.

(29) Kingery, A. F.; Allen, H. E. *Toxicol. Environ. Chem.* **1995**, *47*, 155–184.

JP902474Z